ESD-TR-68-200

Technical Note

1968-27

J. A. Weiss

A High-Field Hysteresigraph

24 July 1968

Prepared for the Advanced Research Projects Agency
under Electronic Systems Division Contract AF 19(628)-5167 by

Lincoln Laboratory
MASSACHUSETTS INSTITUTE OF TECHNOLOGY
Lexington, Massachusetts

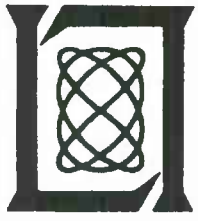

The work reported in this document was performed at Lincoln Laboratory, a center for research operated by Massachusetts Institute of Technology. This research is a part of Project DEFENDER, which is sponsored by the U.S. Advanced Research Projects Agency of the Department of Defense; it is supported by ARPA under Air Force Contract AF 19(628)-5167 (ARPA Order 498).

MASSACHUSETTS INSTITUTE OF TECHNOLOGY
LINCOLN LABORATORY

A HIGH-FIELD HYSTERESIGRAPH

J. A. WEISS

Group 44

TECHNICAL NOTE 1968-27

24 JULY 1968

LEXINGTON MASSACHUSETTS

ABSTRACT

An instrument has been designed for the examination of the switching and hysteresis properties of ferrites intended for use in microwave devices of the "latching" type. The hysteresigraph presents hysteresis loops at audio frequencies, in a form suitable for accurate measurement of magnetization properties. The maximum magnetic field amplitude available is normally about 500 oersteds, which is large compared with the coercive fields of typical materials. Design and performance of the electromagnet, sensing apparatus, and integrating circuits are discussed, and representative data are presented.

Accepted for the Air Force
Franklin C. Hudson
Chief, Lincoln Laboratory Office

CONTENTS

A HIGH-FIELD HYSTERESIGRAPH

I. INTRODUCTION

Magnetic materials of the type generally used in microwave applications, broadly classified as ferrites and iron garnets, may be briefly characterized as follows. Saturation magnetization $4\pi M_s$ ranges up to about 5000 gauss. The coercive field is normally about one oersted, ranging up to 10 oersteds; the remanence ratio M_r/M_s varies widely, normally ranging up to about 0.75; an unusual value of 0.81 has been observed. This ratio, and the "squareness" character of the hysteresis loop, are sensitive to the details of composition and processing. Curie temperatures range up to about 675 °C.

In conventional microwave devices of the fixed-field type, such as circulators and isolators, the character of the magnetization curve is of little consequence, except for its temperature-dependence. Variable devices, on the other hand, such as variable phase shifters (phasers) and attenuators, often involve considerable effort with regard to the selection or development of material having suitable magnetization properties. The most successful of these variable devices have been those incorporating the remanence, or "latching" principle, whereby the ferrite specimen is arranged to form a closed magnetic circuit, or a part of such a circuit, which may be placed in one or the other of its two states of remanent magnetization by means of a current pulse of short duration. This style of operation offers the substantial advantages of possessing a well-reproducible set of states and of requiring a minimum amount of actuating power. The limitation of discreteness may not be a disadvantage if the device is to be used in a microwave system which is controlled by digital logic. Certain devices, such as switches and reversible circulators, are, of course, inherently digital in nature. Another control principle, known as "flux drive," has been devised for use in certain applications, whereby the magnetic circuit may be reproducibly latched in any one of a series of states of partial magnetization. This arrangement, which is in a sense intermediate between remanence and continuous control, makes use of the properties of minor hysteresis loops as well as those of the major loop.

For stability and efficiency in operation of a latching ferrite microwave device, materials are required which fulfill a rather intricate combination of specifications relating to both switching characteristics and microwave response. Study of these materials often requires that data be obtained on the high-field range of the magnetization curve as well as on low-field details of major and minor hysteresis loops, using a single specimen. "Squareness" and other features of the loops relate directly to the latching properties of the device under consideration, while study of the approach to saturation yields an accurate value of saturation magnetization as well as other valuable data relating to microwave performance.[1]

Determination of the magnetization up to high values of applied field poses the following problem. While a toroidal specimen offers the advantage that the internal magnetic field is easily determined, the maximum field obtainable without resorting to difficult experimental techniques is less than 100 oersteds, while in the case of some polycrystalline materials, a state of magnetization within a few percent of saturation may be achieved only at fields upwards of 1000 oersteds. The specimen must be placed in the intense field of an electromagnet; in this situation, the determination of the internal field becomes a major difficulty.

The hysteresigraph to be described here incorporates an electromagnet which can be excited by an AC source in the audio-frequency range, thus permitting both field and flux to be accurately determined with the use of relatively simple integrating circuits. For the sensing of internal field, a magnetic potentiometer designed for audio-frequency operation is used. The flux and field signals are processed by means of operational-amplifier integration circuits and a subtraction stage, resulting in the presentation of magnetization $4\pi M$ vs internal field H.

The hysteresis loop is presented as an oscilloscope trace, which is convenient for qualitative examination. The features of expanded scales and a chopper-modulated reference voltage are used to obtain accurate quantitative data.

Figure 1 shows the arrangement of the electromagnet and magnetic potentiometer. For visibility in the photograph, a nonmagnetic "blank," used

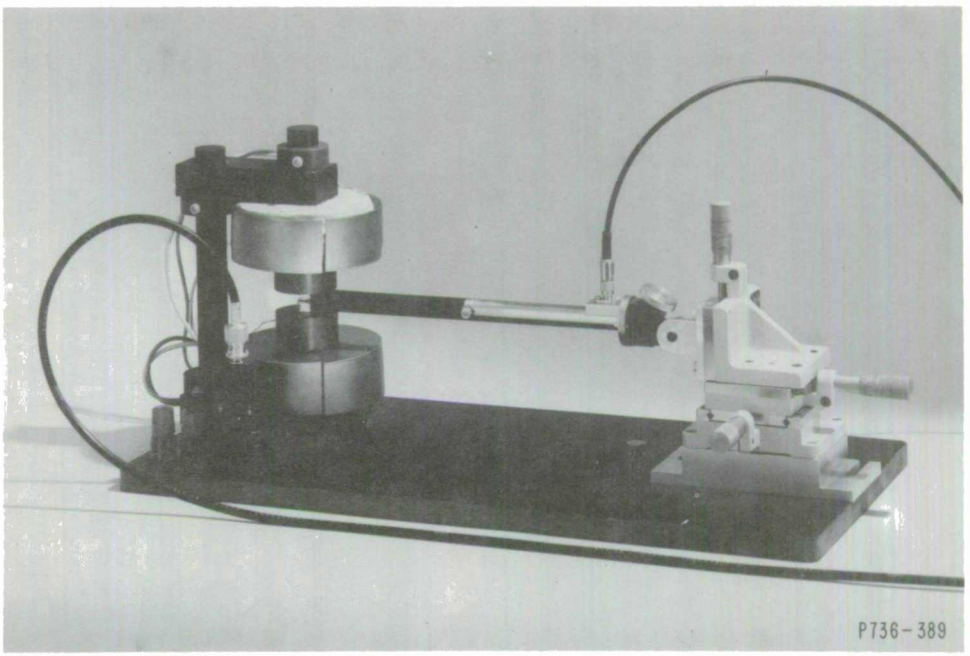

Fig. 1. Photograph of magnet and magnetic potentiometer assembly.

for calibration purposes, has been substituted for the ferrite specimen. In addition to the apparatus shown in the figure, the system includes a magnet power supply, signal-processing unit, and oscilloscope.

The following discussion presents details of the electromagnet, magnetic potentiometer, integration, and subtraction circuits, and oscilloscope presentation. Representative data are included, referring to a number of material types frequently used in microwave devices.

II. ELECTROMAGNET

The requirement, for observation of high-field hysteresis loops of typical ferrite specimens, is a magnet which furnishes fields of at least 500 oersteds with good uniformity over a working region of approximately a half-inch cubed, and which can be excited at audio frequencies in the range below one kHz. We use a commercial nickel-zinc ferrite of saturation magnetization 5000 gauss, coercive field approximately one oersted.

The magnet is shown in Figs. 2 and 3. The yoke is composed of simple cylindrical and rectangular shapes which present no special machining

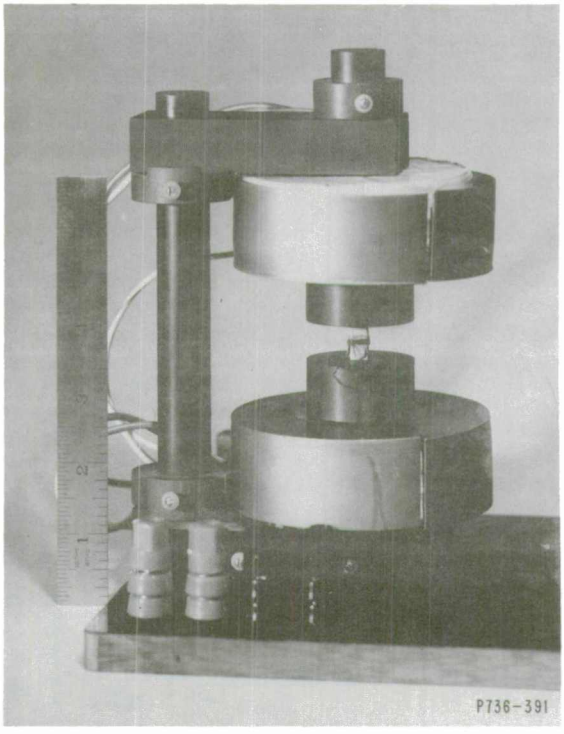

Fig. 2. Photograph of audio-frequency electromagnet.

problems. The cylindrical core of the upper pole piece slides vertically to allow adjustment of the air-gap length from zero to one inch.

The magnet coils are placed immediately above and below the working region to minimize flux leakage, and are designed to be excited by readily available audio-frequency sources. A 60-Hz autotransformer is suitable; when higher or variable frequencies are desired, a 400-Hz motor-generator or an audio oscillator and power amplifier has been used. Each coil consists of 600 turns of No. 17 magnet wire. With the coils in parallel, the DC resistance is 0.7 ohm and the inductance of the electromagnet is 72 mH.

A simple estimate of the field amplitude H_p (peak) in an air gap of length g is

$$H_p = \frac{N}{g} I_p \quad , \tag{1}$$

where N is the number of turns and I_p is peak current. For g = 0.5 inch, this gives $H_p/I_p = 1190$ oe amp^{-1}. At this flux level, the permeability of the material is still sufficiently high to justify the approximation of low reluctance: remanent magnetization of this material is 2700 gauss.

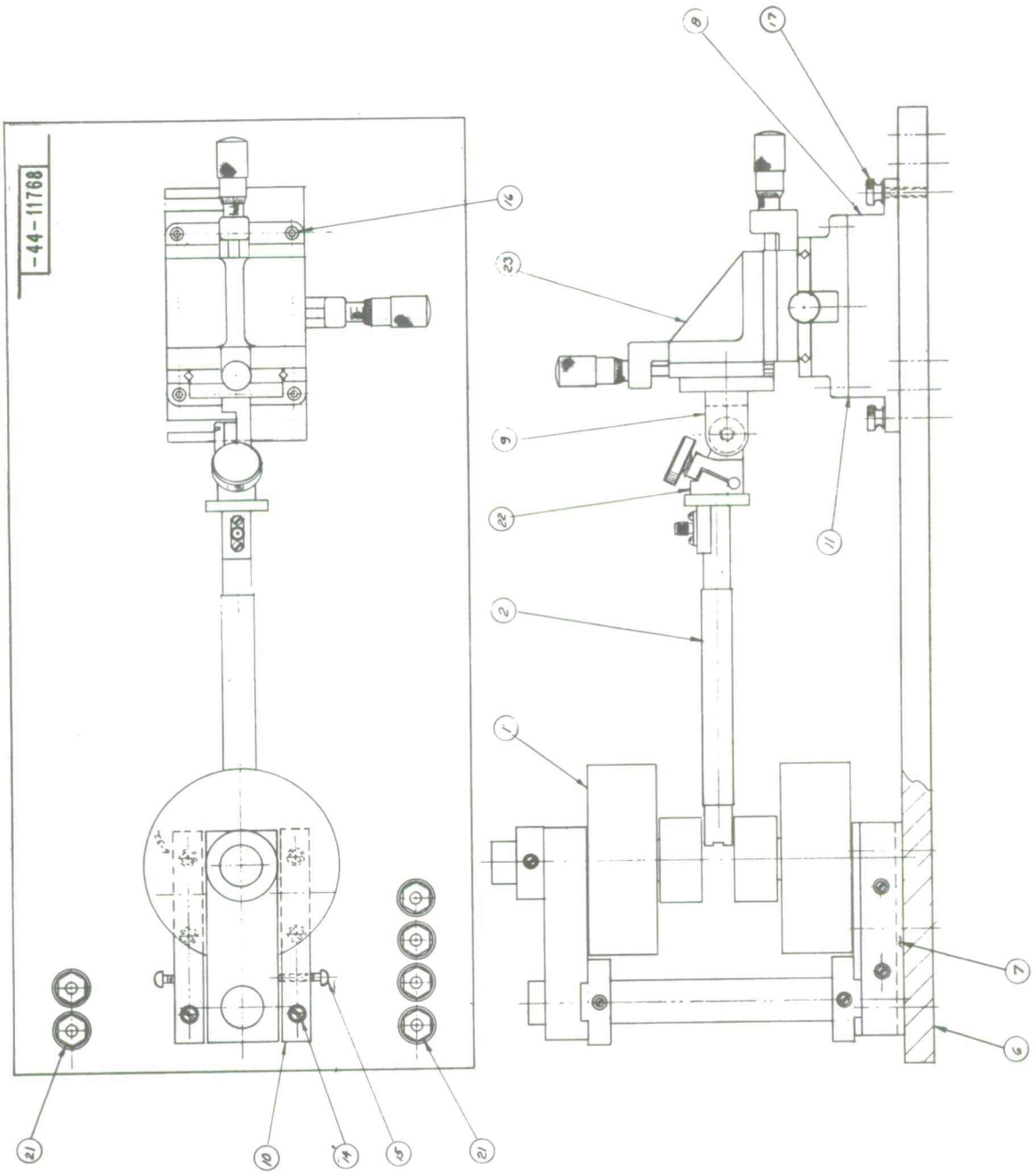

Fig. 3. Assembly drawing of magnet and magnetic potentiometer.

The diameter of the cylindrical core is 0.75 inch. To create an ample region of uniform field, the magnet is furnished with cylindrical pole caps 1.5 inches in diameter. This step in diameter reduces the field by about a factor of four. We predict 278 oe amp^{-1}; thus at $I_p = 2.5$ amp, the predicted field is 745 oersteds. The observed field is 559 oersteds, which is in reasonable agreement with the simple formula, when the reluctance of the yoke and the effects of fringing and residual air gaps are considered.

Resistive heating of the windings is negligible. Some hysteresis heating is noticeable when the magnet is operated for long periods above $I_p \sim 3$ amp. At high fields, the magnetostrictive hum is perceptible.

III. MAGNETIC POTENTIOMETER

According to Bates,[2] the principle of the magnetic potentiometer was originally suggested by A. P. Chattock in 1887 (hence the instrument is sometimes called a Chattock potentiometer) and was later proposed independently by W. Rogowski.

The objective of the instrument is to generate a signal which yields as accurately as possible a measure of the effective internal field in the specimen. If the specimen is uniformly magnetized, then the tangential field just inside the side surface is representative of this field and, by virtue of the requirement of continuity, the tangential field just outside this surface is representative also. In general, the field varies rapidly with increasing distance outside the specimen surface. Hence, the accuracy of the measurement depends on our ability to sense the field at the very surface. Effects which influence the variation of the field in the vicinity of the specimen are the finite permeability of the magnet material, finite diameter of the pole pieces, and the presence of air gaps between the pole pieces and the end faces of the specimen.

The magnetic potentiometer accomplishes the objective of sensing the tangential field at the surface. More precisely, as its name indicates, it senses the magnetic potential difference between two points on the surface. To illustrate the principle, we consider a long, thin solenoid consisting of

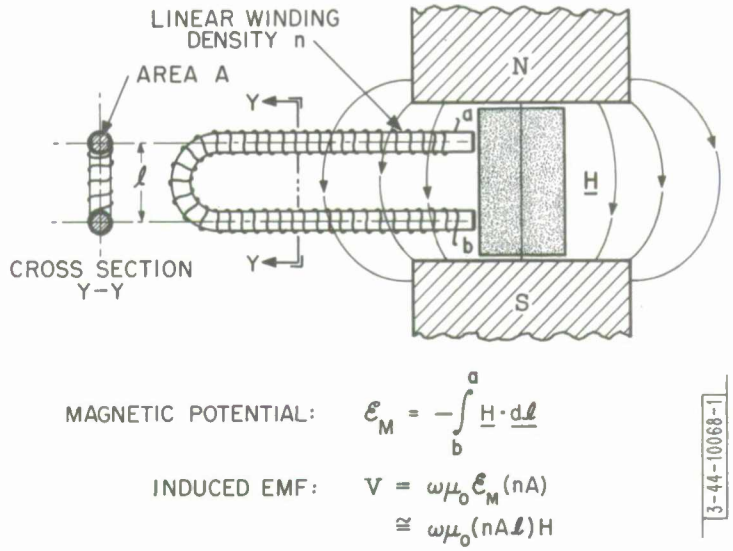

Fig. 4. Magnetic potentiometer principle.

many turns of fine wire wound on a flexible rod, as shown in Fig. 4. Let A denote the cross-sectional area and n the linear winding density (number of turns per unit length). On an element of length of the solenoid axis whose magnitude and direction are represented by the vector $\underline{dl}$, the number of turns is ndl. In a time-varying field $\underline{H}$ the EMF induced in this element is

$$dV = -\mu_o nA\underline{dl} \cdot \frac{d}{dt} \underline{H} \quad . \tag{2}$$

Thus, the total EMF is

$$V = -\mu_o nA \frac{d}{dt} \int_{\underline{r}_a}^{\underline{r}_b} \underline{H} \cdot \underline{dl} \tag{3}$$

or

$$V = \mu_o nA \frac{d}{dt} F_{ab} \quad , \tag{4}$$

where $\underline{r}_a$ and $\underline{r}_b$ are the positions of the ends of the solenoid and F_{ab} is the magnetic potential difference between these two points. In a slowly varying field which is free of conduction currents, however, F_{ab} is independent of the

path of integration. We bend the solenoid into a "hairpin" shape with its ends distance d apart. F_{ab} is the magnetic potential difference between the ends; if the field is uniform, we have

$$F_{ab} = Hd \quad , \tag{5}$$

where H is the component of field parallel to the line connecting the ends.

For a field which varies sinusoidally in time at angular frequency ω, the amplitudes of V_p and H_p are connected by

$$V_p = \mu_o \omega (nAd) H_p \quad . \tag{6}$$

Thus, the sensitivity of the instrument is characterized by the geometrical factor nAd.

Our embodiment of the magnetic potentiometer follows the above prescription, except for a modification which simplifies construction by avoiding the operation of bending the solenoid. To meet the requirement of a nonconducting core, a polyimide plastic was selected which has favorable mechanical properties, especially machinability to close tolerances. Two rods, each 5.5 inches long, were centerless-ground to 0.0625-inch diameter. Each was wound with two layers of No. 44 magnet wire (copper diameter 2 mils) over a 5-inch length. Special attention was given to uniformity of the windings and to bringing one end of the winding flush with the end face of the rod. The two wound rods were installed in a split cylindrical holder with their axes 0.290 inch apart. The holder was assembled, partially enclosed in a steel shield tube, as shown in Figs. 5 and 6, to form the magnetic potentiometer probe. The two windings are connected in series, aiding with respect to a field transverse to the probe axis.

Although the magnetic potentiometer principle envisions a continuous winding over the entire length of the core, it is difficult in practice to form the wound core into the required "hairpin" shape. It is permissible, however, to construct the winding out of two disjointed sections, provided the magnetic potential difference between the separated parts is negligible. The steel tube shown in the figures creates an equipotential region enclosing the electrically

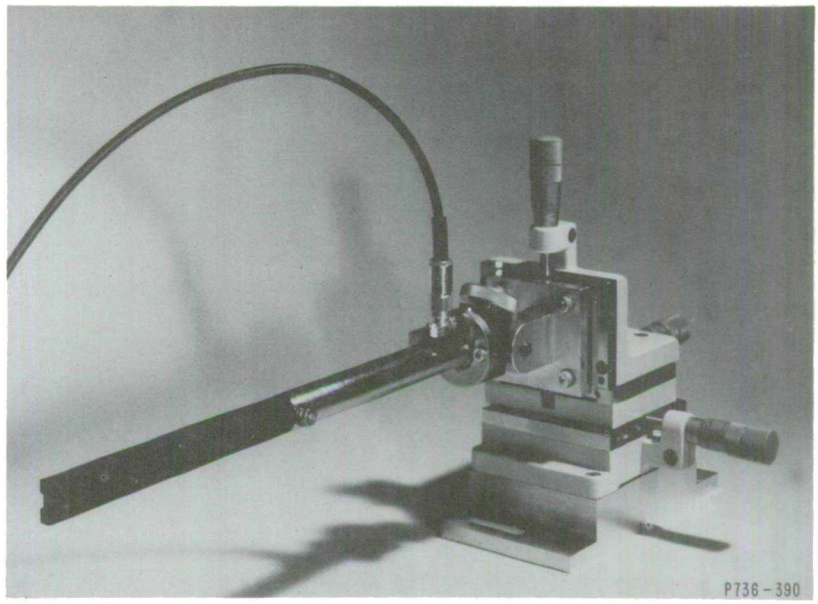

Fig. 5. Magnetic potentiometer probe and mounting.

adjacent ends of the two sections, by virtue of both its magnetic and conducting properties, thereby fulfilling the requirement.

From the geometry of the structure described, we have n = 358 turns cm^{-1} for a two-layer winding. The cross-sectional area A, including the effective thickness of the windings, is A = 0.0227 cm. For the calibration, we predict

$$\frac{\mu_o \omega H_p}{E_p} = \frac{1}{nAd} = 167 \times 10^7 \text{ Tesla (volt/sec)}^{-1} \quad .$$

The experimentally observed values are usually higher than this by about 10 percent, primarily due to slight defects in the uniformity of the winding.

The magnetic potentiometer probe is mounted on a micrometer stage which provides adjustment of position in three dimensions. There is also provision for small adjustments of the direction of the probe axis, thus permitting accurate placement of the sensing end of the probe against the face of the specimen.

IV. INTEGRATION

The open-loop transfer characteristics of an operational amplifier may be represented approximately for our purposes by the factor

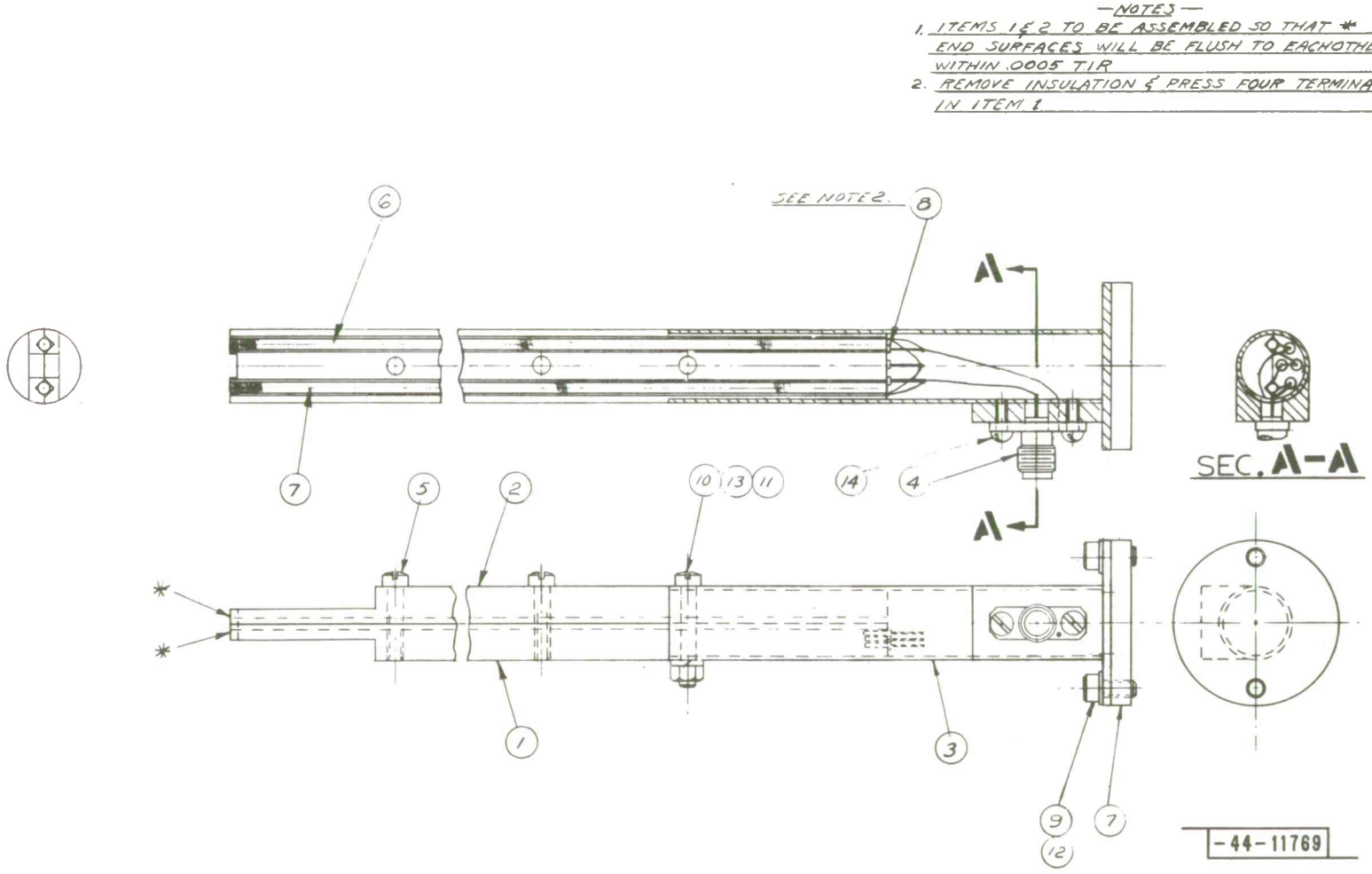

Fig. 6. Assembly drawing of magnetic potentiometer probe.

$$A = A_o \frac{1}{1 + j\omega\tau_A} \quad , \tag{7}$$

where A_o is the DC gain and τ_A is the characteristic roll-off time. For the amplifier used to produce the magnetic-field signal (the H-channel), we have $A_o = 10^6$ (120 dB) and $\tau_A = 0.32$ sec, corresponding to unity-gain frequency of 0.5 MHz. Under the simplest conditions of operational amplifier use, the network includes input impedance Z_i and feedback impedance Z_f. Let $Z_f/Z_i = \zeta$; then the closed-loop transfer characteristic is

$$\frac{e_o}{e_i} = \frac{-\zeta}{(1 + 1/A) + \zeta/A} \quad , \tag{8}$$

where e_i and e_o are the input and output voltage amplitudes, respectively. For integration, $Z_i = R$ and $Z_f = 1/j\omega C$. To obtain accurate integration, we require that deviation of the denominator of Eq. (8) from unity be negligible at all relevant frequencies. With A as given in Eq. (7), and with $RC = 10^{-5}$ sec, this requirement is amply fulfilled up to 0.1 MHz.

The fundamental frequency of the hysteresigraph is in the low audio range — generally 60 or 400 Hz. Under high-field operating conditions, the flux and field signals are rich in harmonics. An estimate of the harmonic content of the signals generated in the magnetic potentiometer and in the flux-sensing winding (proportional to dH/dt and dB/dt, and referred to below as the H- and B-signals, respectively) may be obtained by the following considerations. Consider a substantially square-loop material whose coercive field is about one oersted, excited at 400 Hz with field amplitude of, say, 500 oersteds. The major part (domain-wall displacement) of the magnetization reversal would occur in about 5 μsec if the driving source possessed "constant-field" characteristics; i.e., if the time-dependence of the field were sinusoidal and independent of the behavior of the magnet and specimen. In that case, the H-signal would contain only the 400-Hz fundamental; the B-signal is a train of 5-μsec pulses, as illustrated in Fig. 7(a), whose corresponding spectrum would be centered at about 100 kHz. In practice, the volume of typical specimens is such that the magnet and its source experience a substantial loading effect:

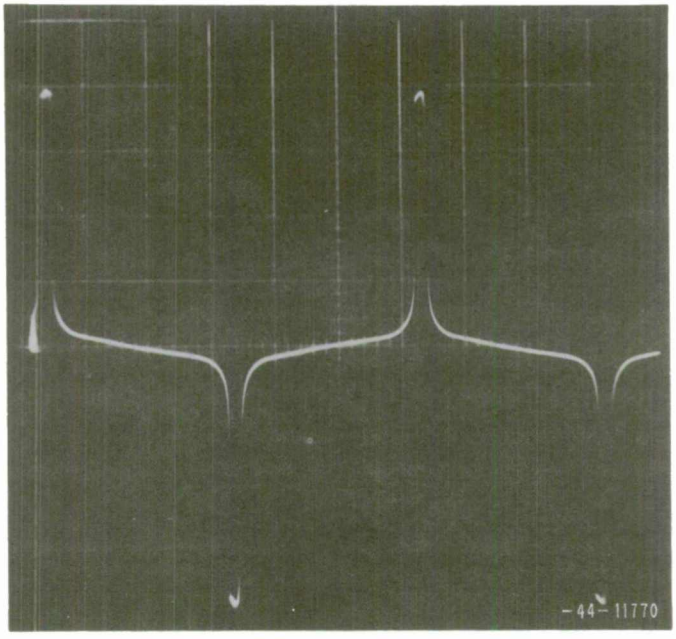

Fig. 7(a). Oscillogram: dB/dt vs t, 400 Hz.

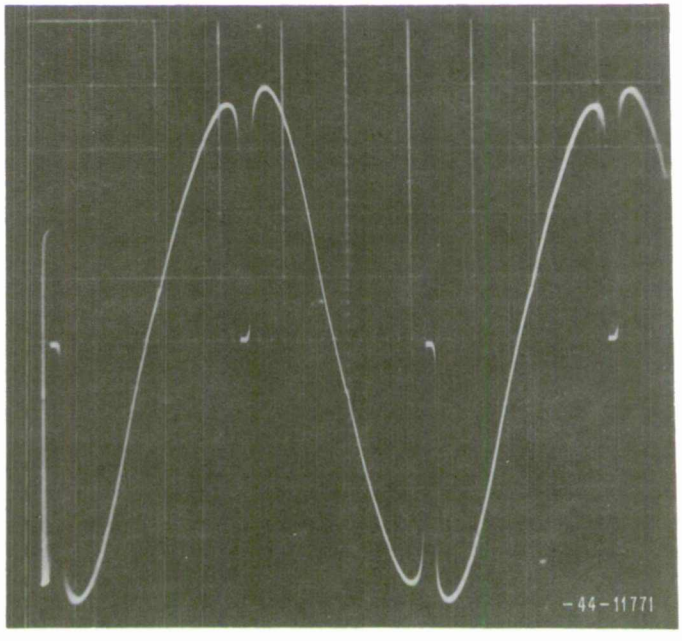

Fig. 7(b) Oscillogram: dH/dt vs t, 400 Hz.

during the major magnetization reversal process, the specimen acts momentarily as a magnetic "short circuit" which stalls the variation of the field. The time duration of this part of the process is consequently prolonged, ranging from 5 to 25 μsec, depending on the material and specimen size. The effect is that the spectrum is displaced to somewhat lower frequencies; in addition, a narrow pulse is introduced into the H-signal, where dH/dt momentarily drops from its maximum to a small value, as illustrated in Fig. 7(b). The spectral content of this pulse is similar to that of the B-signal, but errors in the processing of this signal produce more obvious distortions of the hysteresis loop, particularly in the presentation of coercivity.

In principle, there would be no difficulty in performing accurate integrations of the signals described above if the characteristics of the operational amplifiers conformed to the ideal expression, Eq. (8). In reality, however, the noise and voltage and current offset which are inevitably present result in more or less erratic drift of the output voltage. The problem is to suppress these effects in such a way as to introduce a minimum amount of distortion of the hysteresis-loop presentation.

The solution, developed by F. Betts,[3] consists of a drift-suppression network incorporated in the feedback network of each integrator, as shown in Fig. 8, together with a filter for suppression of high-frequency noise, placed at the output. Analysis of the integrator, including the effects of these networks, shows that at frequencies well below 60 Hz, integration is disabled, while at 60 Hz, the deviation from ideal integration is no greater than one part in 1.4×10^3 in amplitude, and one part in 5.4×10^5, or 1.1×10^{-4} degrees, in phase. At higher frequencies, the deviation becomes negligible. To indicate the relevance of this phase deviation value, we note that, under the operating conditions contemplated above, an error in the phase relation between the 400-Hz components of the B- and H-signals in the amount of 0.36 degrees would result in an error of 100 percent in the measurement of coercive field.

The integrated B- and H-signals are shown in Figs. 9(a) and 9(b). Since we are usually more interested in the properties of the magnetization $4\pi M$ than in the induction B, the outputs of the B- and H-channels are combined in

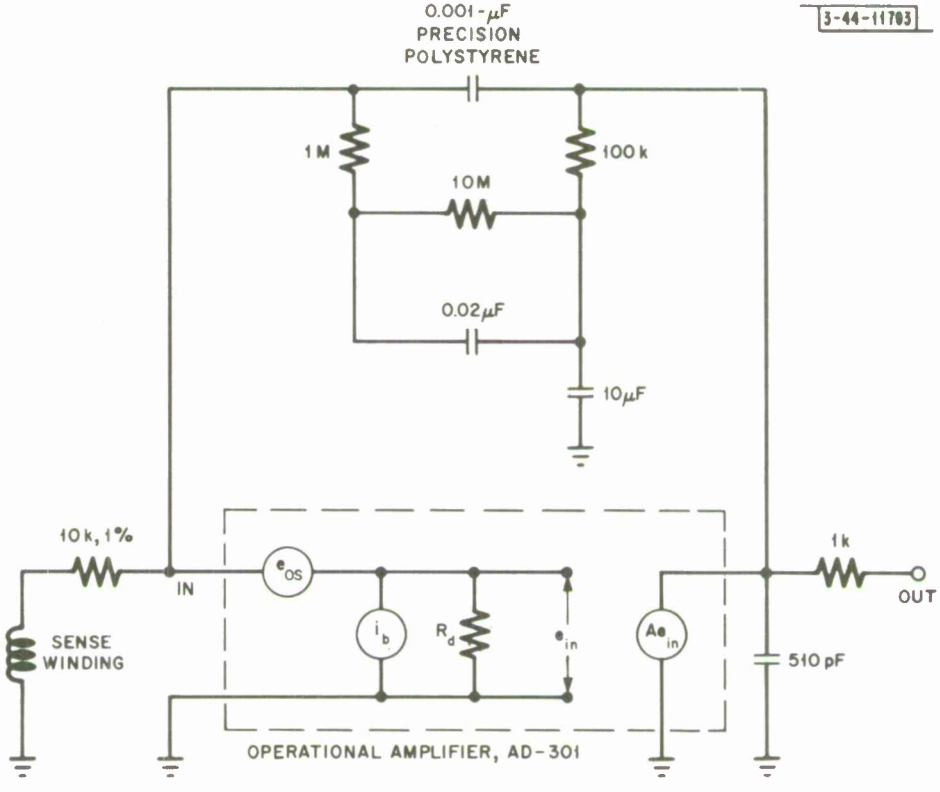

Fig. 8. Circuit diagram of H-channel integrator stage, with drift-suppression network and noise filter.

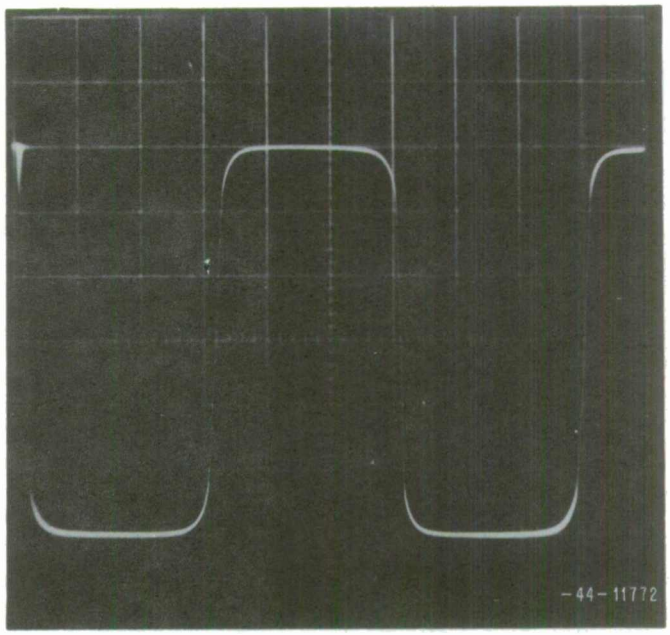

Fig. 9(a). Oscillogram: B vs t, 400 Hz.

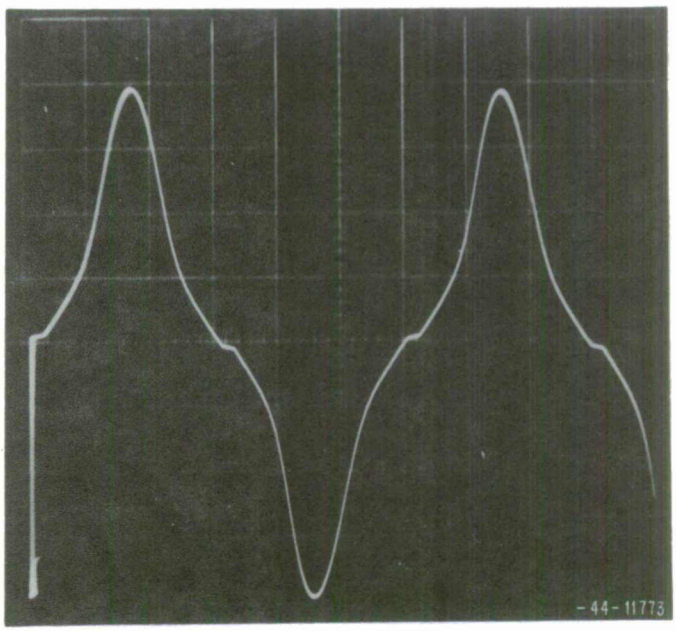

Fig. 9(b). Oscillogram: H vs t, 400 Hz.

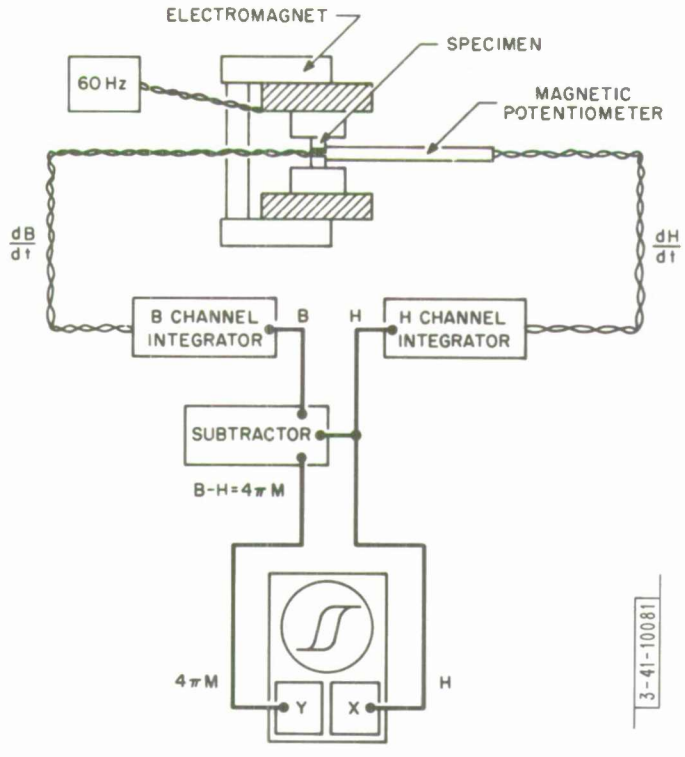

Fig. 10. Block diagram of hysteresigraph.

a difference stage, as indicated in the block diagram, Fig. 10. The resulting hysteresis loop of a typical material, a gadolinium-aluminum substituted yttrium-iron garnet whose saturation magnetization is 745 gauss, is shown in full in Fig. 11(a), and on an expanded scale in Fig. 11(b).

For calibration purposes, a nonmagnetic "blank" specimen having the same dimensions as the specimen under study is substituted; the two inputs to the difference stage are adjusted for null output. In the presence of the magnetic specimen, the output is then proportional to $4\pi M$.

V. PRESENTATION – CALIBRATION

Presentation of the hysteresis loop is in the form of an oscilloscope trace. To minimize errors in the phase relation between the vertical ($4\pi M$) and horizontal (H) signals, we use an XY-oscilloscope with amplifier units of the same type in both the X and Y channels. For detailed examination of the loops, it is convenient to use a type of plug-in unit which provides a calibrated expansion of scale and a calibrated DC reference voltage.

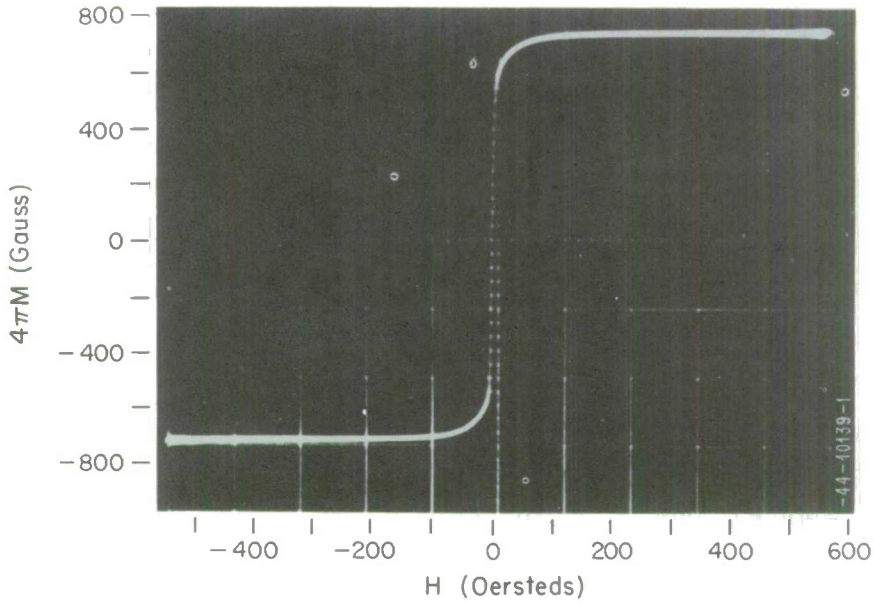

Fig. 11(a). Hysteresis loop of a microwave garnet, $4\pi M_s$ = 745 gauss.

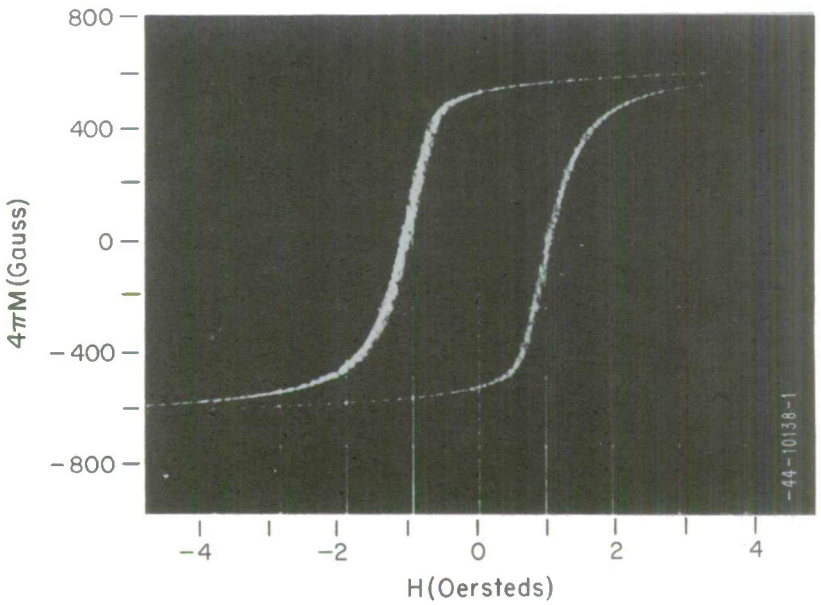

Fig. 11(b). Hysteresis loop on an expanded scale.

For convenience in the measurement of remanent magnetization, coercive field, and other details, we use a chopper to interrupt the DC reference voltage at about a 20-Hz rate, thereby producing a double image of the loop, the two images being relatively displaced by an adjustable amount in either the X or Y direction. Figure 12 shows a typical hysteresis loop (a lithium ferrite; $4\pi M_s \sim 3750$ gauss, $H_c \sim 3$ oe): (a) in full with field amplitude 516 oersteds; (b) on an expanded horizontal scale; (c) chopped horizontally for measurement of coercive field; and (d) chopped vertically for measurement of remanent magnetization.

The chopper was designed by J. DiBartolo. One is installed permanently within each plug-in unit. A circuit diagram is shown in Fig. 13.

Calibration of the field and flux channels is performed with the aid of a nonmagnetic "blank" specimen of the same dimensions as those of the material to be investigated and wound with the same B-sensing coil. Typical specimen dimensions are 0.250×0.250 inch in cross section and 0.550 inch long. When the nonmagnetic material is in place, there is no loading effect on the magnet and its source; hence, the field is accurately sinusoidal if the source is. Measurement of the signal induced in the B-sensing winding, together with measurement of the cross-sectional area of the winding and the frequency of the source, determines the field. By measuring the same field with the magnetic potentiometer, we determine the calibration of this instrument. The calibration corresponding to the value given in Sec. III is 1.67×10^7 oersteds $(\text{volt sec})^{-1}$, or 6.01×10^{-8} volt sec $(\text{oersted})^{-1}$. When the magnetic potentiometer is used in combination with an integrator of the type discussed in Sec. IV, having time constant $\tau = 10^{-5}$ sec, the combination yields 167 oersteds $(\text{volt})^{-1}$, or 6.00 mV $(\text{oersted})^{-1}$. The magnetic potentiometer may also be used to determine the uniformity of the field over the region to be occupied by the specimen; depending, however, on the size and magnetic character of the specimen, the field configuration may change substantially, of course, when it is introduced.

The adjustment of the two inputs to the difference stage is also performed with the aid of the nonmagnetic specimen. The accuracy with which the difference between the values of H as detected by the B-sensing winding and by the

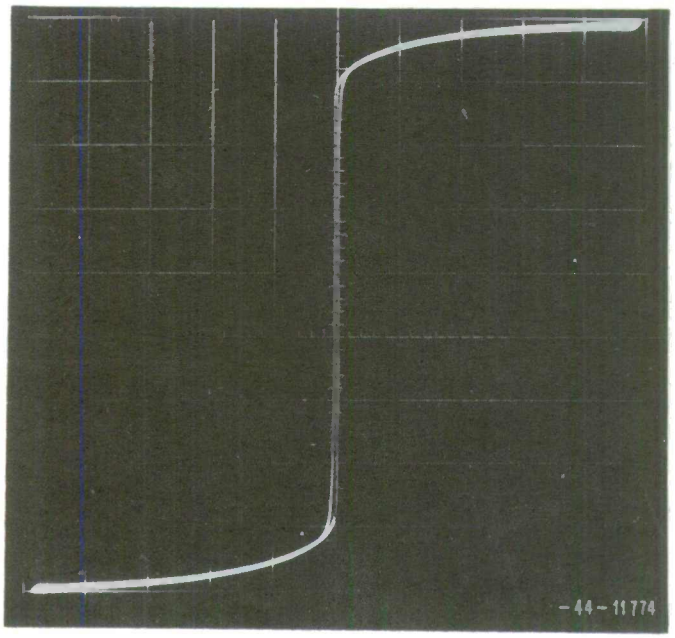

Fig. 12(a). Hysteresis loop of a lithium ferrite, field amplitude 516 oersteds.

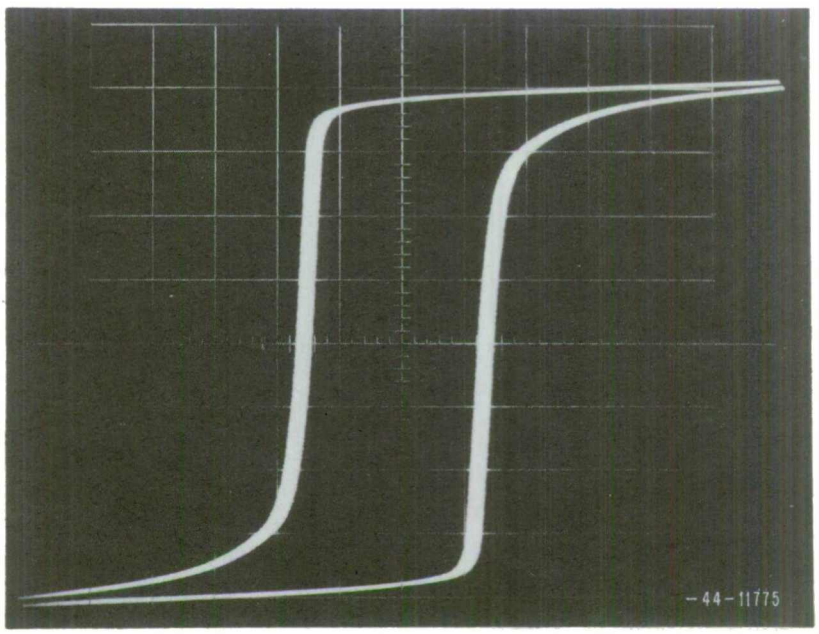

Fig. 12(b). Hysteresis loop of a lithium ferrite, expanded.

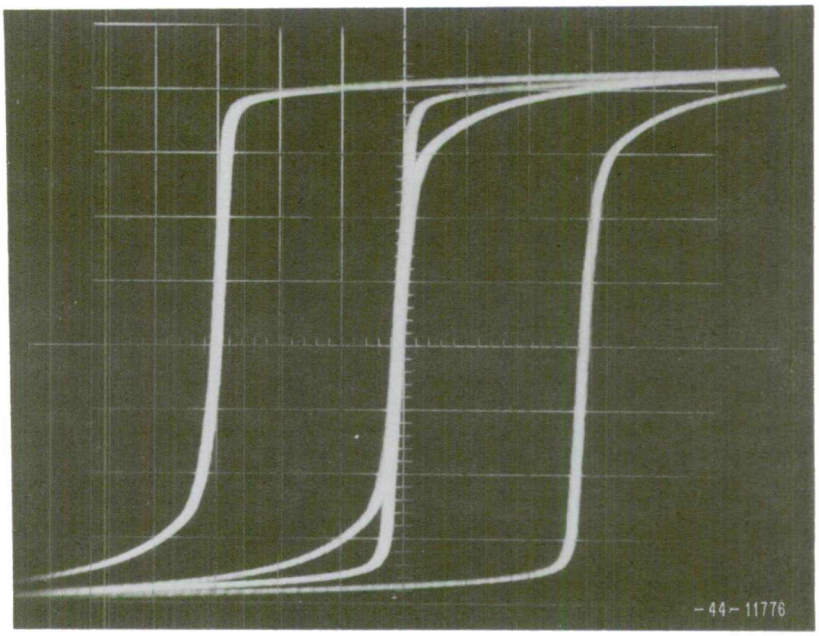

Fig. 12(c). Loop of Fig. 12(a), chopped for observation of coercive field.

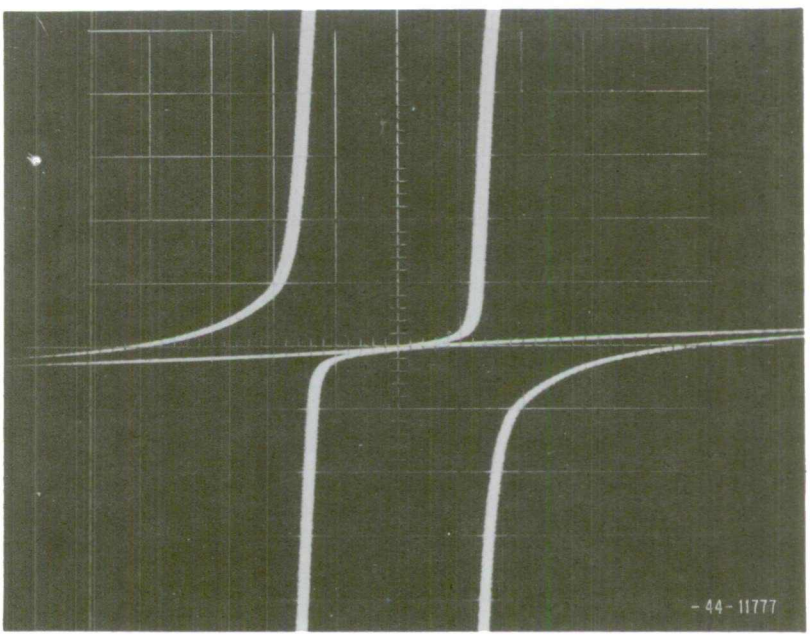

Fig. 12(d). Loop of Fig. 12(a), chopped for observation of remanent magnetization.

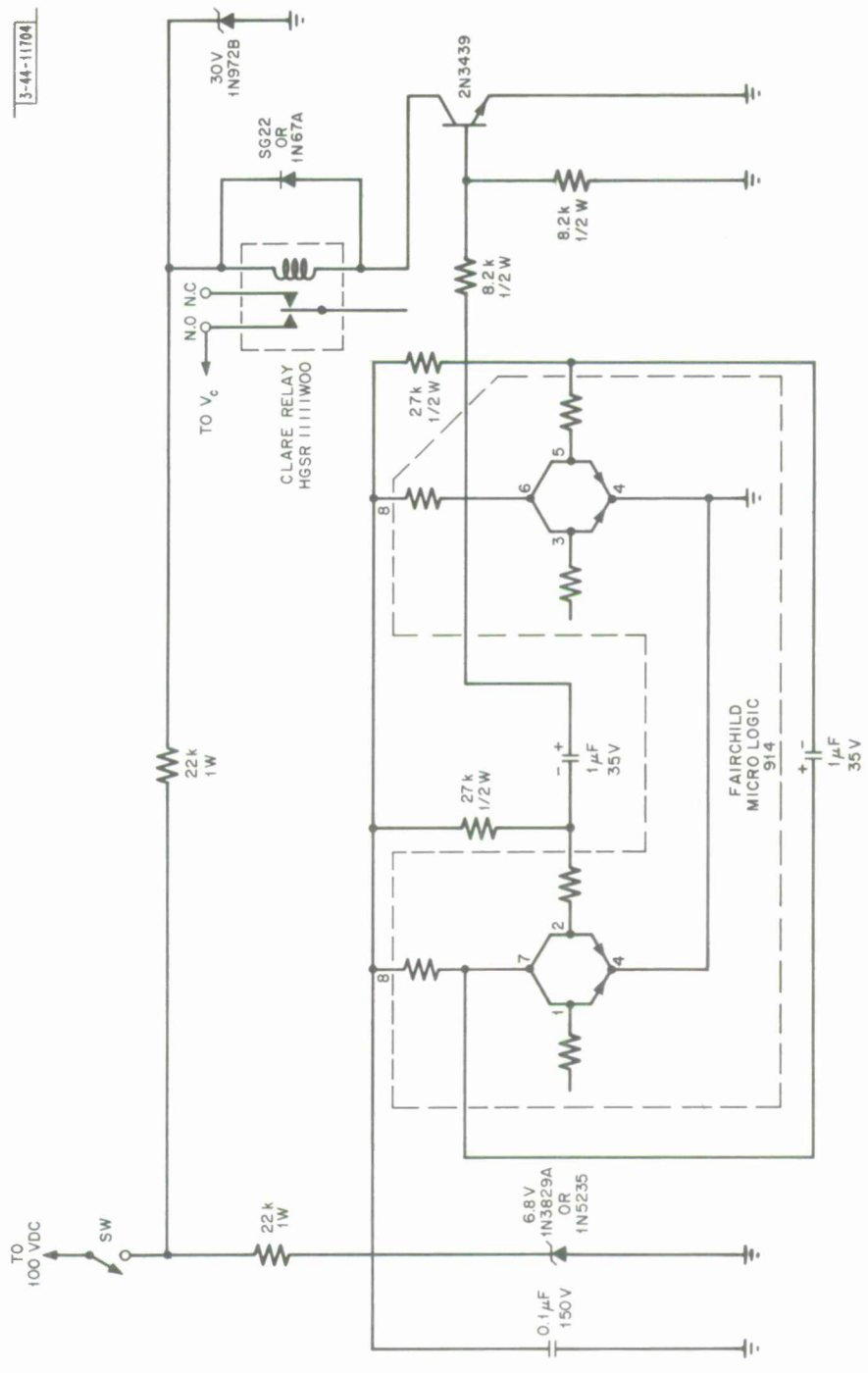

Fig. 13. Circuit diagram of chopper for oscillograph display.

the magnetic potentiometer can be reduced to zero is limited only by the noise in the two channels.

Calibration of the B-channel for accurate measurement of magnetization is rather troublesome, due in part to uncertainties in the determination of the effective area of the B-sensing winding. A calibration procedure using the remanent magnetization of a standard material as a reference has been successfully used. The standard specimen is cut from a material whose remanent magnetization has been well established from the hysteresis loop of a second piece accurately machined in the shape of a thin-walled toroid. When the toroid is uniformly wound with primary and secondary windings, and excited by a current which produces a field of at least five times the coercive field of the material, an accurate and reproducible value of remanent magnetization can be obtained from the output of a carefully calibrated integrator, together with the number of turns of the secondary winding and the area of the flux path. With a standard specimen of this type, only the cross-sectional area of the sample itself is important, and not that of the B-sensing winding.

VI. REPRESENTATIVE DATA

Figures 14 through 22 are hysteresis loops, in full and expanded, of each of nine materials of types frequently used in microwave device design. Values of maximum magnetization, remanent magnetization, remanence ratio, and coercive field, as measured with the hysteresigraph, are presented.

REFERENCES

1. G. F. Dionne (M.I.T. Lincoln Laboratory), "Determination of Magnetic Anisotropy and Porosity from the Approach to Saturation of Polycrystalline Ferrites" (to be published).
2. L. F. Bates, Modern Magnetism (Cambridge University Press, London, 1951).
3. J. A. Weiss and F. Betts, "Hysteresis Evaluation of Microwave Ferrites at Audio Frequency with Large Dynamic Range," J. Appl. Phys. 38, 1397 (March 1, 1967).

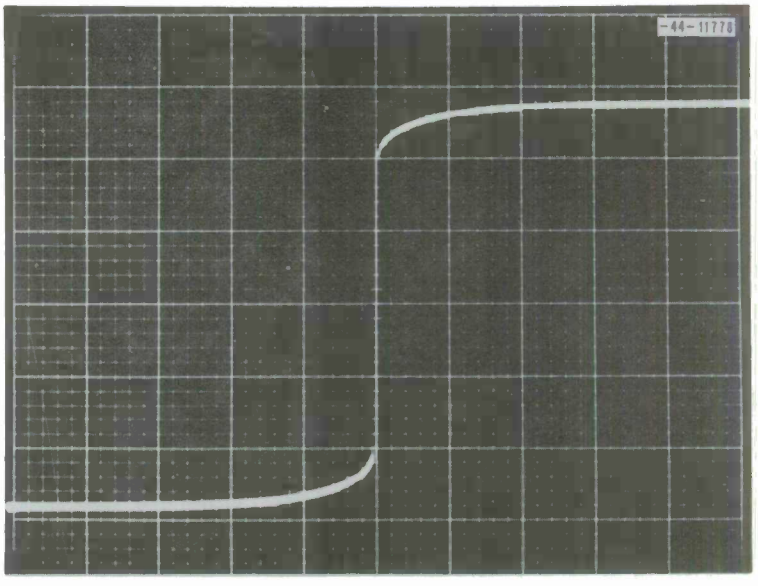

Fig. 14(a). Material No. 1, MgMn ferrite; $4\pi M_{max}$ = 1681 gauss; $4\pi M_{rem}$ = 1252 gauss; M_{rem}/M_{max} = 0.745; H_c = 1.3 oersteds; $H_{max} \cong$ 560 oersteds (high).

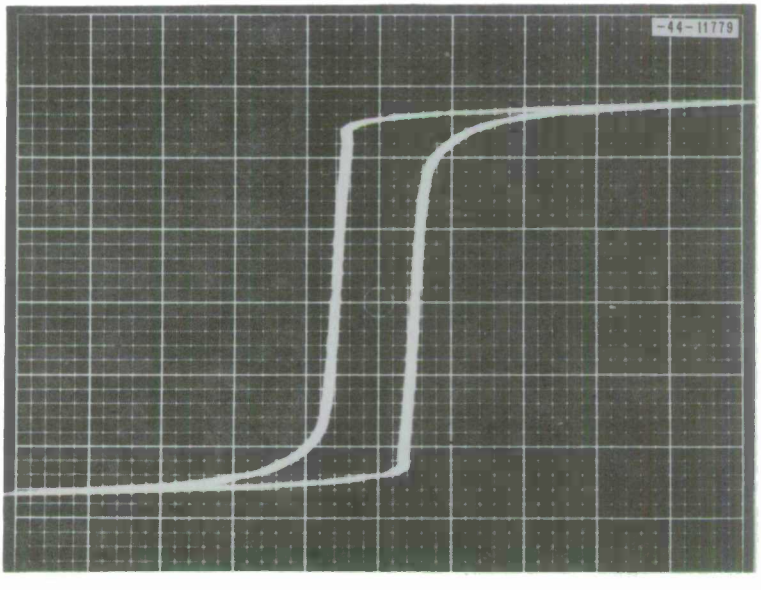

Fig. 14(b). Same as Fig. 14(a) except low-field scale.

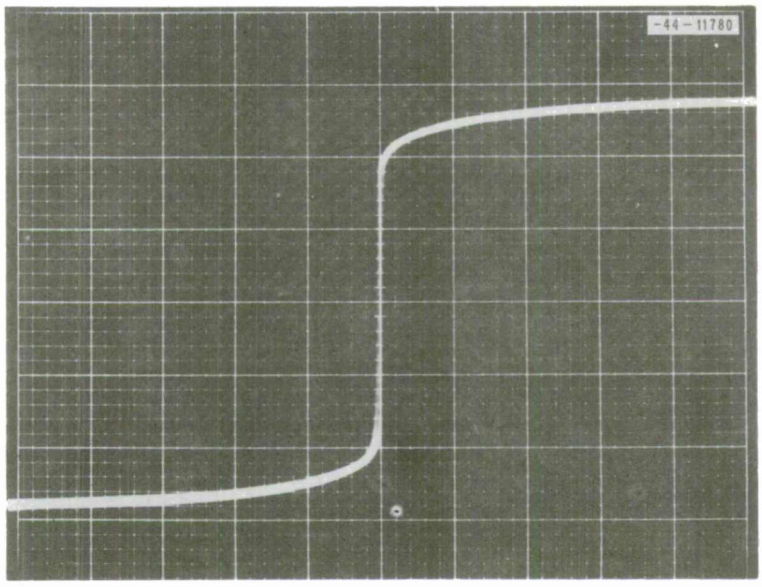

Fig. 15(a). Material No. 2, MgMn ferrite; $4\pi M_{max}$ = 2040 gauss; $4\pi M_{rem}$ = 1400 gauss; M_{rem}/M_{max} = 0.685; H_c = 2.0 oersteds; $H_{max} \cong$ 560 oersteds (high).

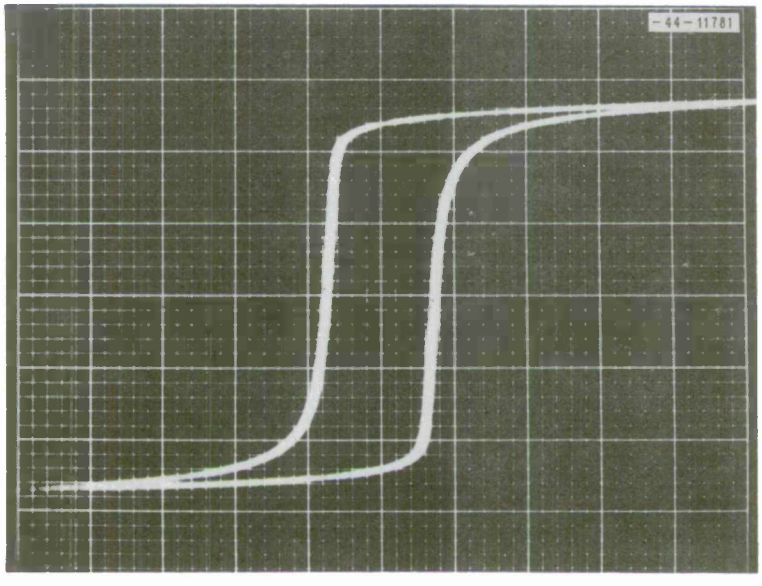

Fig. 15(b). Same as Fig. 15(a) except low-field scale.

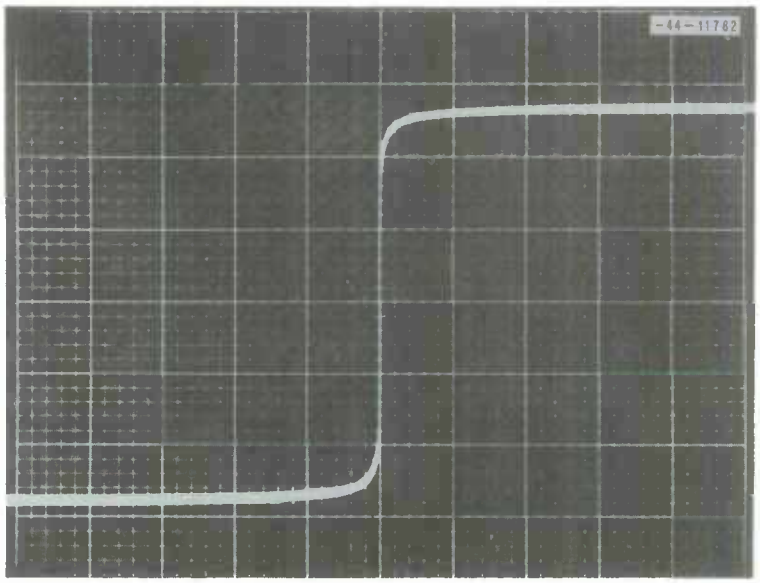

Fig. 16(a). Material No. 3, MgMn ferrite; $4\pi M_{max}$ = 712 gauss; $4\pi M_{rem}$ = 484 gauss; M_{rem}/M_{max} = 0.680; H_c = 0.4 oersted; $H_{max} \cong$ 560 oersteds (high).

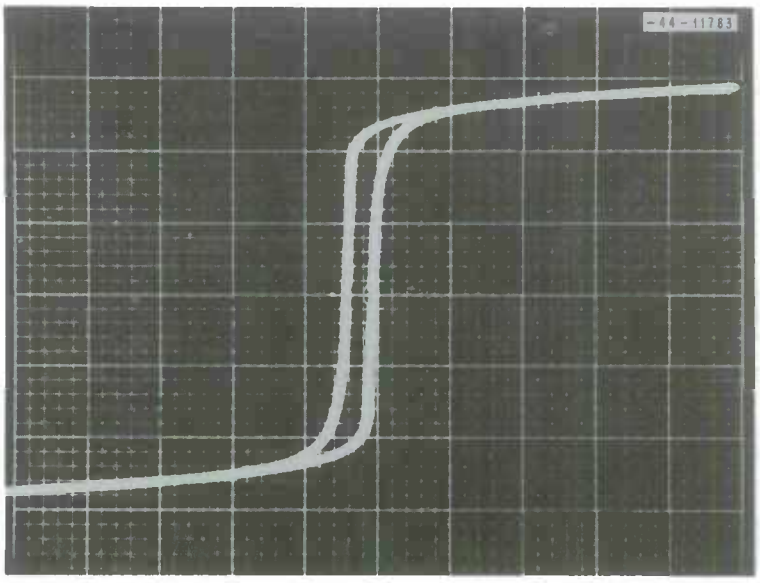

Fig. 16(b). Same as Fig. 16(a) except low-field scale.

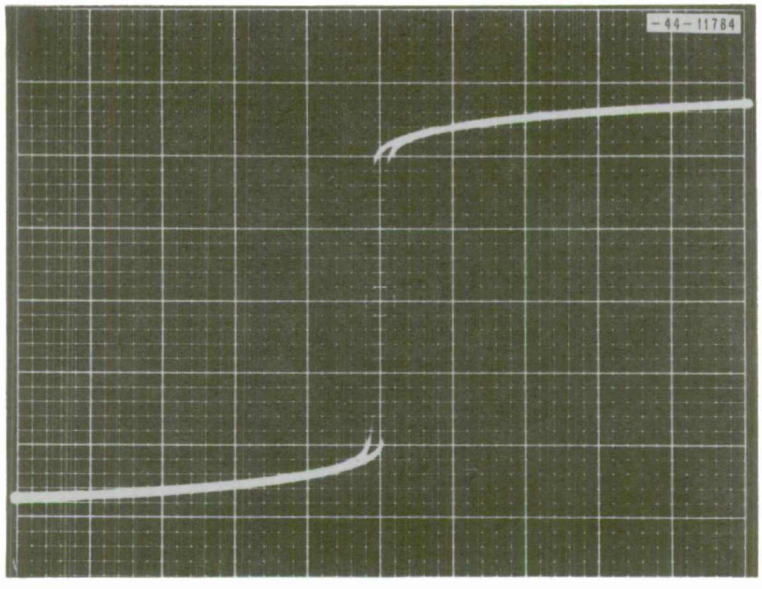

Fig. 17(a). Material No. 4, NiCo ferrite; $4\pi M_{max}$ = 2780 gauss; $4\pi M_{rem}$ = 2020 gauss; M_{rem}/M_{max} = 0.727; H_c = 5.7 oersteds; $H_{max} \cong$ 560 oersteds (high).

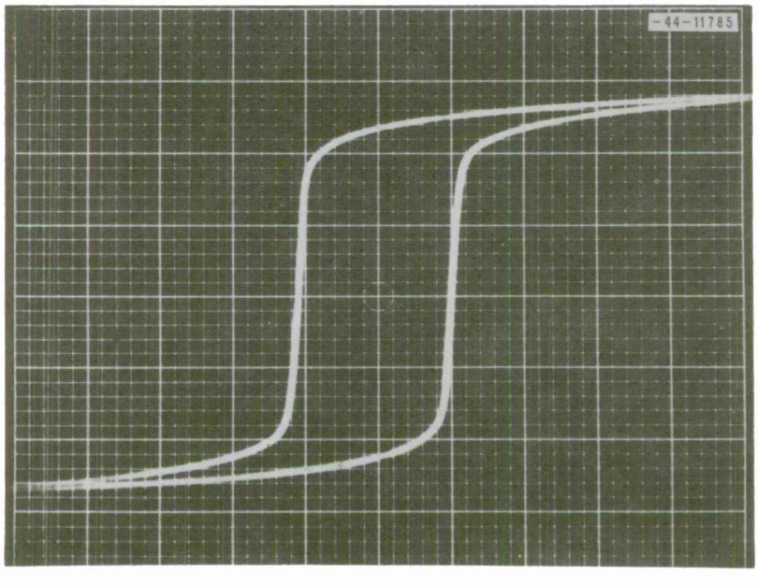

Fig. 17(b). Same as Fig. 17(a) except low-field scale.

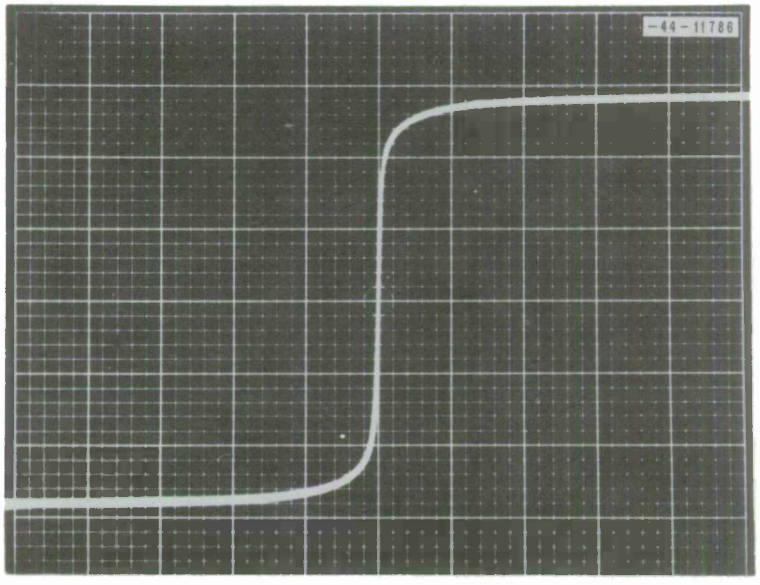

Fig. 18(a). Material No. 5, NiZn ferrite; $4\pi M_{max}$ = 4780 gauss; $4\pi M_{rem}$ = 1770 gauss; M_{rem}/M_{max} = 0.371; H_c = 0.7 oersted; $H_{max} \cong$ 560 oersteds (high).

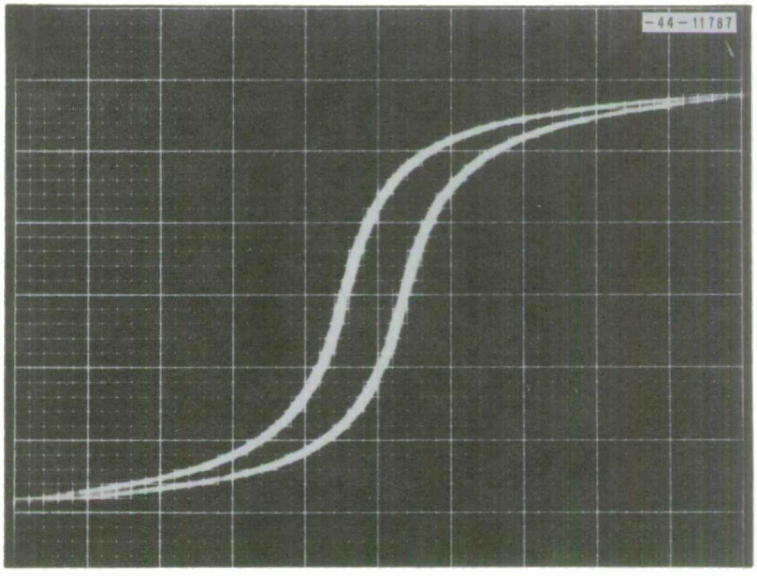

Fig. 18(b). Same as Fig. 18(a) except low-field scale.

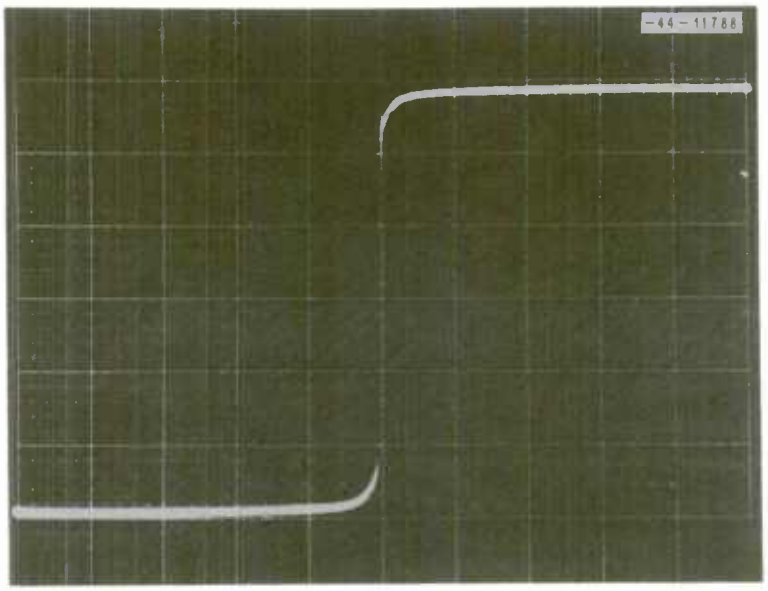

Fig. 19(a). Material No. 6, AlYIG ferrite; $4\pi M_{max}$ = 418 gauss; $4\pi M_{rem}$ = 300 gauss; M_{rem}/M_{max} = 717; H_c = 0.7 oersted; $H_{max} \cong$ 560 oersteds (high).

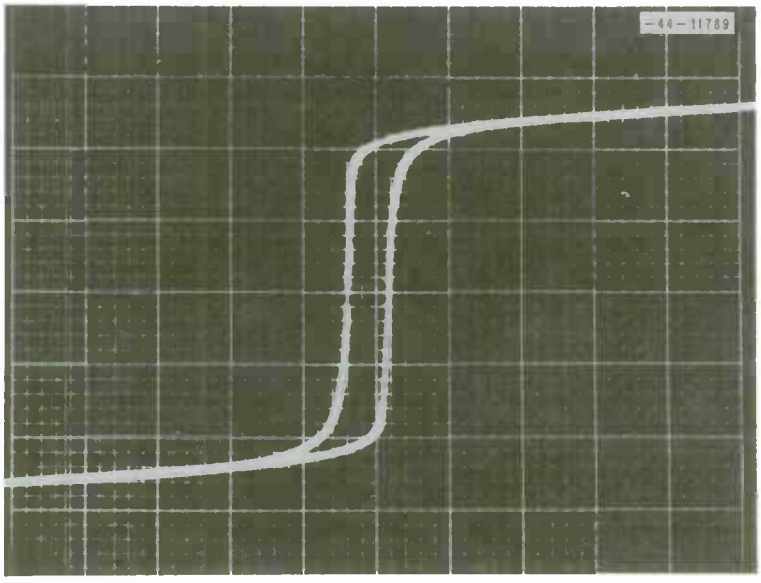

Fig. 19(b). Same as Fig. 19(a) except low-field scale.

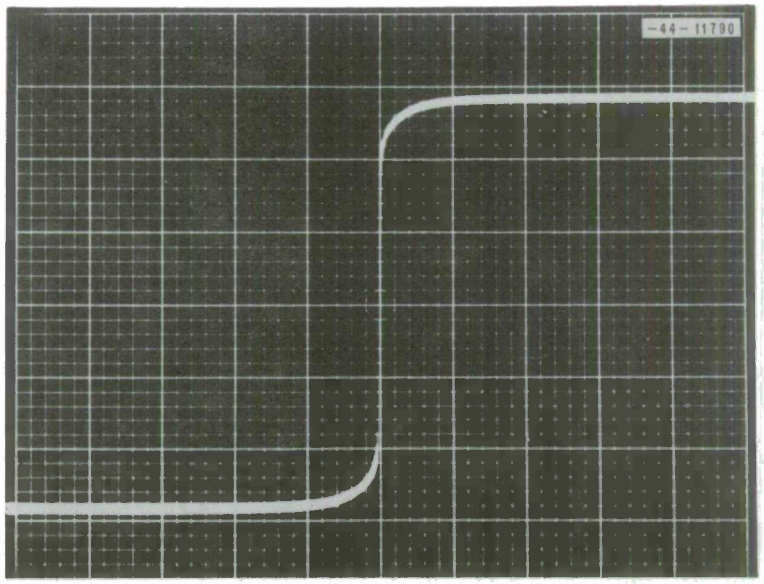

Fig. 20(a). Material No. 7, GdAlYIG ferrite; $4\pi M_{max}$ = 791 gauss; $4\pi M_{rem}$ = 522 gauss; M_{rem}/M_{max} = 660; H_c = 0.7 oersted; $H_{max} \cong$ 560 oersteds (high).

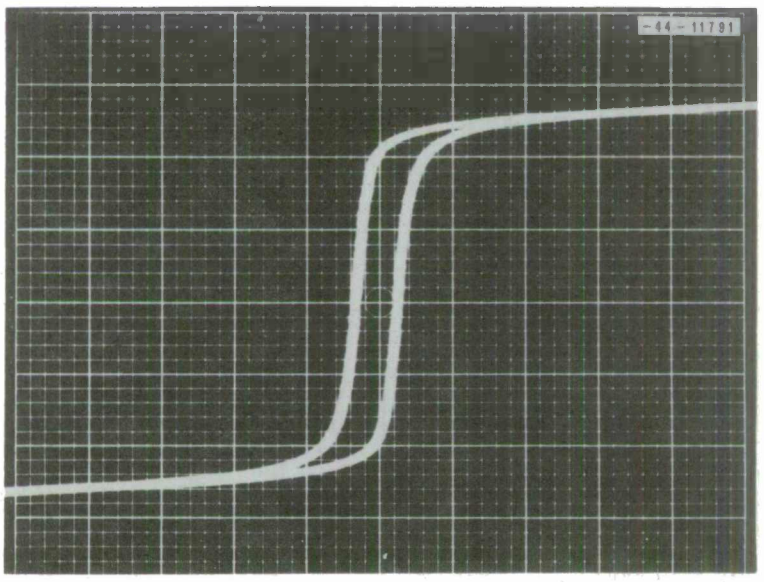

Fig. 20(b). Same as Fig. 20(a) except low-field scale.

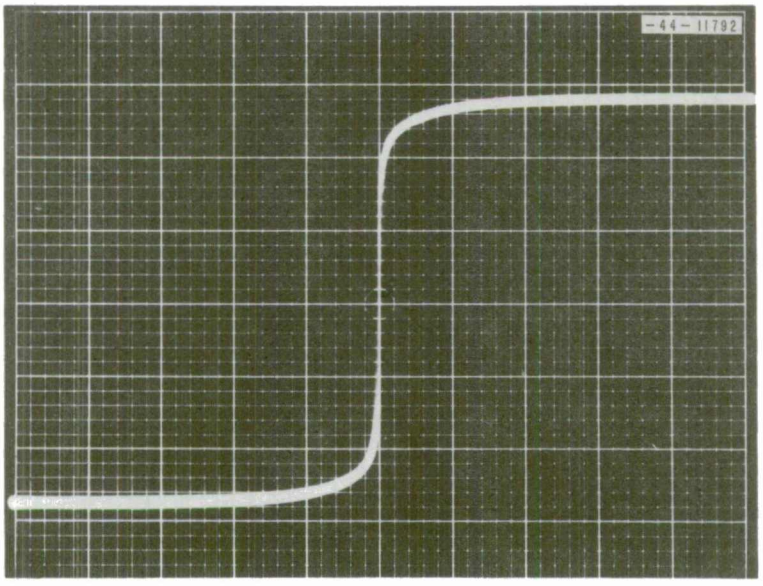

Fig. 21(a). Material No. 8, GdYIG ferrite; $4\pi M_{max}$ = 695 gauss; $4\pi M_{rem}$ = 414 gauss; M_{rem}/M_{max} = 596; H_c = 2.0 oersteds; $H_{max} \cong$ 560 oersteds (high).

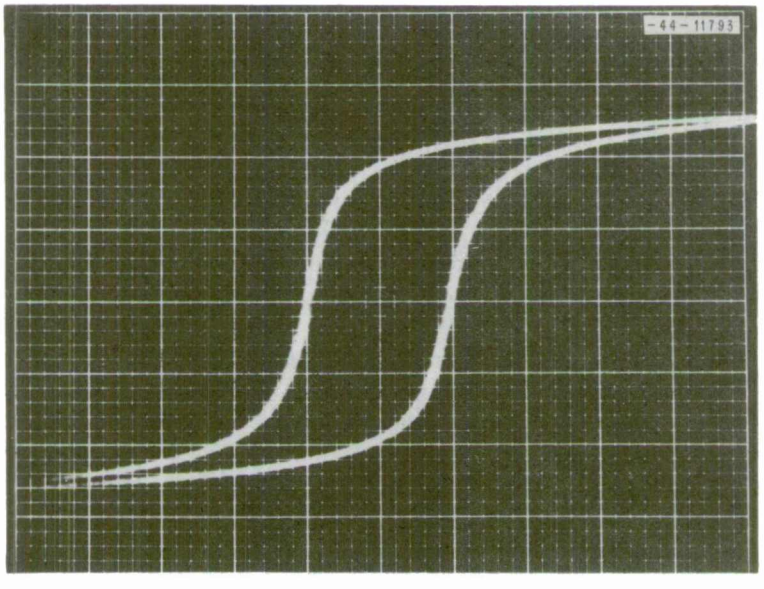

Fig. 21(b). Same as Fig. 21(a) except low-field scale.

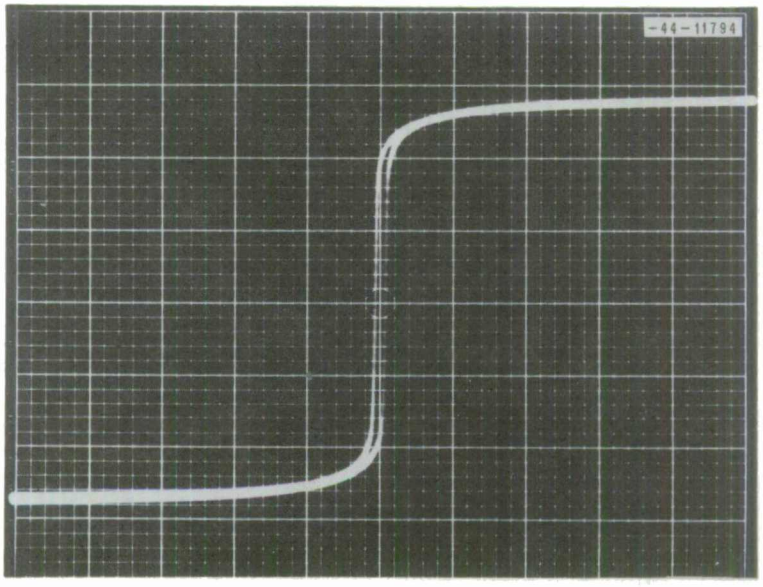

Fig. 22(a). Material No. 9, LiAl ferrite; $4\pi M_{max}$ = 1530 gauss; $4\pi M_{rem}$ = 1168 gauss; M_{rem}/M_{max} = 764; H_c = 5.2 oersteds; $H_{max} \cong$ 560 oersteds (high).

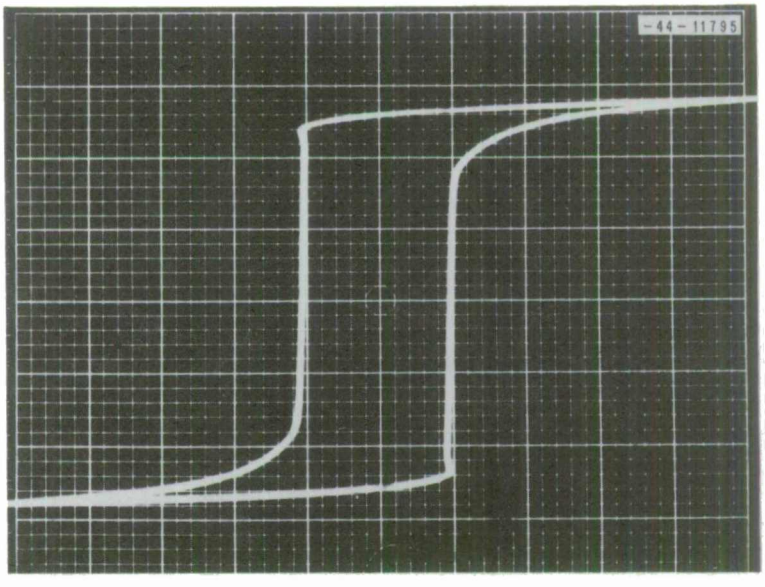

Fig. 22(b). Same as Fig. 22(a) except low-field scale.

DOCUMENT CONTROL DATA – R&D

(Security classification of title, body of abstract and indexing annotation must be entered when the overall report is classified)

1. ORIGINATING ACTIVITY *(Corporate author)* Lincoln Laboratory, M.I.T.	2a. REPORT SECURITY CLASSIFICATION Unclassified 2b. GROUP None

3. REPORT TITLE

A High-Field Hysteresigraph

4. DESCRIPTIVE NOTES *(Type of report and inclusive dates)*

Technical Note

5. AUTHOR(S) *(Last name, first name, initial)*

Weiss, Jerald A.

6. REPORT DATE	7a. TOTAL NO. OF PAGES	7b. NO. OF REFS
24 July 1968	36	3

8a. CONTRACT OR GRANT NO. AF 19(628)-5167 b. PROJECT NO. ARPA Order 498 c. d.	9a. ORIGINATOR'S REPORT NUMBER(S) Technical Note 1968-27 9b. OTHER REPORT NO(S) *(Any other numbers that may be assigned this report)* ESD-TR-68-200

10. AVAILABILITY/LIMITATION NOTICES

This document has been approved for public release and sale; its distribution is unlimited.

11. SUPPLEMENTARY NOTES	12. SPONSORING MILITARY ACTIVITY
None	Advanced Research Projects Agency, Department of Defense

13. ABSTRACT

An instrument has been designed for the examination of the switching and hysteresis properties of ferrites intended for use in microwave devices of the "latching" type. The hysteresigraph presents hysteresis loops at audio frequencies, in a form suitable for accurate measurement of magnetization properties. The maximum magnetic field amplitude available is normally about 500 oersteds, which is large compared with the coercive fields of typical materials. Design and performance of the electromagnet, sensing apparatus, and integrating circuits are discussed, and representative data are presented.

14. KEY WORDS

hysteresigraph
ferrites
microwave devices
magnetic fields
electromagnets
sensing apparatus
potentiometers